Journal of Information & Computational Science 10:5 (2013) 1377–1389 March 20, 2013
Available at http://www.joics.com

3D B Spline Interval Wavelet Moments for 3D Objects ⋆

Li Cui [a,*], Ying Li [b]

[a] *School of Mathematical Sciences, Laboratory of Mathematics and Complex Systems, Ministry of Education, Beijing Normal University, Beijing 100875, China*

[b] *College of Computer Science and Technology, Jilin University, Changchun 130021, China*

Abstract

By introducing B spline interval wavelets to the 3D wavelet moments, we give a new representation for 3D objects. The new descriptors can keep more information of the edge. They are invariant to translation, rotation and scale, and have the multi-resolution features in the radial direction, which can handle noise to some extent and provide multi-level features to satisfy various requirements. With the Pearson correlation coefficient and the energy in each level, we give a new method to measure the similarity of two objects. In the experiment, it is proved to be an efficient method.

Keywords: B Spline Interval Wavelets; Moments; Spherical Harmonics; Pearson Correlation Coefficient

1 Introduction

With the development of 3D CAD, games, and web application etc., more and more 3D models pour into our life. It demands an efficient retrieval system to recognize similar objects for further decision. For shape descriptors of 3D objects, there are several methods, such as shape distribution [15], reflective symmetry descriptors [9], 3D Fourier descriptors [10], spherical harmonics descriptors [11] and 3D Zernike moments [13], etc. Here, 3D Zernike moments, as the extension of 2D Zernike moments, are invariant to rotation, are complete in $L^2(R^3)$ and have no redundant information. We have extended the 2D wavelet moments to the 3D case by introducing the spherical harmonics together with the wavelet function in [3]. They are invariant to rotation and have the multi-level trait, which are consistent with the 2D wavelet moments. Moreover they overcome the complex computation of high order Zernike moments and have the advantage on identification of the similar objects. In the past, with Mallat algorithm of the wavelets and fractal scale, we have given fractal scale descriptors based on 2D wavelet moments for gait sequence. They are proved to be an efficient method in gait recognition [4, 14]. Furthermore the combination of Mallat algorithm and fractal scale is shown as a good method in 3D objects recognition [5]. While the objects in reality are finite and the edge of objects are more important, it is natural to

⋆Project supported by the National Nature Science Foundation of China (No. 11001017).

*Corresponding author.
Email address: licui@bnu.edu.cn (Li Cui).

1548–7741 / Copyright © 2013 Binary Information Press
DOI: 10.12733/jics20101578

consider the wavelets on the interval in the 3D wavelet moments. In 1993, Cohen and Daubechies present wavelets on the interval [2], which can directly be constructed by the classical orthonormal wavelets, specially by Daubechies wavelets. The generalized Mallat algorithm still holds. So we introduce the Daubechies interval wavelets on $[0, 1]$ in 3D wavelet moments in our paper [6]. However the B spline wavelets are more efficient in pattern recognition field. Quak and Weyric presented the B spline interval wavelets and give the algorithm in [16], which are more suitable to character objects. Replacing the Daubechies interval wavelets to B spline wavelets is meaningful in practice.

Furthermore, since the wavelets are used, the new descriptors contain low-pass and high-pass part, which are very different in energy. Only using Euclidean distance to measure the similarity of two objects could ignore the different in high-pass part. Pearson correlation coefficient is known as a better method to measure two vectors with different scale. It measures the strength and direction of a linear relationship between the two vectors [8]. In this paper, we try to get weighed Pearson correlation coefficient according their decomposition level and energy. Moreover together with the globe Pearson correlation coefficient of the descriptors, we get a new distance which is called Pearson distance of two objects.

In this paper, we develop 3D B spline interval wavelet moments by using B spline wavelets on the interval [0, 1], which maintain the edge of the objects. In the following paper we recall the definition and general computation step of 3D wavelet moments. Then we list the mean idea of wavelets on the interval, give the new definition of 3D B spline interval wavelet moments in detail, and together with Mallat algorithm we give the new descriptors of 3D objects. In Section 4, we do some experiments to test our algorithm in a middle database. Finally, some conclusions are shown.

2 3D Wavelet Moments

2.1 Definition of 3D Wavelet Moments

Translation invariant and scaling invariant can be achieved using the geometric moments as follows, like in [7].

The (p, q, r) degree geometric moments of $f(x, y, z)$ defined on field Ω are

$$m_{pqr} = \int\int\int_{\Omega} x^p y^q z^r f(x, y, z) dx dy dz, p, q, r \in N.$$

Since the center of the shape is invariant to translation, rotation and scale, the method of solving the translation problem is to locate the centroid of the object. The coordinates of the center (X_0, Y_0, Z_0) are

$$X_0 = m_{100}/m_{000}, Y_0 = m_{010}/m_{000}, Z_0 = m_{001}/m_{000}.$$

The scaling factor of the present object size, compared with the expected constant size V_0 is $\alpha = \sqrt[3]{m_{000}/V_0}$. In this way, we can obtain the translation and scale normalized shape by changing the coordinates according to the transformation

$$\begin{pmatrix} x \\ y \\ z \end{pmatrix} \rightarrow \begin{pmatrix} (x - X_0)/\alpha \\ (y - Y_0)/\alpha \\ (z - Z_0)/\alpha \end{pmatrix}.$$

Let $f(x,y,z)$ represent a 3D object in the (x,y,z)-coordinate, and its corresponding form in the polar coordinate is $\tilde{f}(r,\theta,\phi)$. The relationship between $f(x,y,z)$ and $\tilde{f}(r,\theta,\phi)$ is given by

$$x = r\cos(\theta)\sin(\phi), y = r\sin(\theta)\sin(\phi), z = r\cos(\phi),$$

where $r \in [0,\infty), \theta \in [0,2\pi], \phi \in [0,\pi]$.

In the rest of our paper, for convenience suppose $f(x,y,z)$ and $f(r,\phi,\theta)$ respectively represent a normalized object f in Cartesian and polar coordinate.

The spherical harmonics is used to get rotation invariant moments like in 3D Zernike moments.

Definition 1 *[3] Suppose $\psi(r)$ is a wavelet function, $f(r,\phi,\theta)$ is normalized 3D object defined on field Ω. Its 3D wavelet moments are*

$$F_{pqlm}^{wavelets} = \int\int\int_{\Omega} f(r,\phi,\theta)\psi_{pq}(r)\overline{Y_l^m(\phi,\theta)}r^2\sin(\phi)drd\phi d\theta, \tag{1}$$

where $\psi_{pq}(r) = 2^{p/2}\psi(2^p r - q), p,q \in Z$, $Y_l^m(\phi,\theta)$ is the spherical harmonics, $-l \le m \le l, l \in N, m \in Z$.

Here spherical harmonics $Y_l^m(\phi,\theta)$ is given by

$$Y_l^m(\phi,\theta) = N_l^m P_l^m(\cos(\phi))\exp(im\theta),$$

where N_l^m is a normalization factor

$$N_l^m = \sqrt{\frac{(2l+1)(l-m)!}{4\pi(l+m)!}},$$

and $P_l^m(x)$ denotes the associated Legendre functions,

$$P_l^m(x) = (1-x^2)^{m/2}\frac{d^m}{dx^m}P_l(x),$$

where $P_l(x) = \frac{1}{2^l l!}\frac{d^l}{dx^l}(x^2-1)^l$ is Legendre polynomial.

The vector of spherical harmonics $\mathbf{Y}_l = (Y_l^l, Y_l^{l-1}, H\cdots, Y_l^{-l})^T$ for a given l forms the basis of a $(2l+1)$-dimensional subspace, which is invariant under the options of the full rotation group [13]. Then let $\mathbf{F}_{pl} = (F_{pll}, F_{pl(l-1)}, \cdots, F_{pl(-l)})^T$, the L^2-norm $\|\mathbf{F}_{pl}\|_2$ is invariant to the rotation.

As a result, 3D wavelet moments descriptors $\{\|\mathbf{F}_{pl}\|_2\}_{pl}$ are invariant to translation, scaling and rotation.

2.2 Completeness and Computation of the Wavelet Moments

By introduce wavelet, the wavelet moments can represent the object $f \in L^2(R^3)$[3].

Theorem 1 *[3] Suppose $\Psi_{pqlm}(r,\phi,\theta) = \frac{1}{r}\psi_{pq}(r)\overline{Y_l^m(\phi,\theta)}$, for $p, q \in \mathbf{Z}$, $-l \le m \le l$, $l \in \mathbf{N}$, $m \in \mathbf{Z}$, we get*

$$\langle \Psi_{pqlm}, \Psi_{p'q'l'm'} \rangle = \delta_{pp'}\delta_{qq'}\delta_{ll'}\delta_{mm'},$$

$$f = \sum_{p\in Z}\sum_{q\in Z}\sum_{l=0}^{\infty}\sum_{m=-l}^{l}\langle f, \overline{\Psi}_{pqlm}\rangle\overline{\Psi}_{pqlm},$$

where $\langle f, g\rangle = \int\int\int_{R^3} f(r,\phi,\theta)\overline{g(r,\phi,\theta)}r^2\sin(\phi)drd\theta d\phi$

From Theorem 1, the 3D wavelet moments are orthogonal and complete. 3D wavelet moments get the global and local characters and make the complete representation of 3D objects.

Furthermore there exists fast algorithm for the computation of 3D wavelet moments. Suppose

$$S_{lm}(r) = \int_0^{2\pi}\int_0^{\pi} f(r,\phi,\theta)\overline{Y_l^m(\phi,\theta)}\sin(\phi)d\phi d\theta. \tag{2}$$

The computation of $F_{pqlm}^{wavelets}$ can be reduced to compute

$$F_{pqlm}^{wavelets} = \int_0^{\infty} S_{lm}(r)\psi_{pq}(r)r^2dr. \tag{3}$$

The formula (2) can be gained by the fast algorithm of spherical harmonics, which uses the 1D fast Fourier transform and the iteratively fast algorithm of Legendre polynomial [12]. Moreover Mallat algorithm of the wavelets can be used to compute the formula (3). Together with the fast algorithm of formula (2), the computation of 3D wavelet moments invariant is double accelerated. For the computational complexity, they have the superiority over the 3D Zernike moments. The 3D Zernike moments are computed by the weighted sum of the 3D geometric moments and are related to the complexity of their computation [13], while the 3D geometric moments dramatically increase in complexity and are not stabile to noise with increasing order.

3 B Spline Interval Wavelets in 3D Wavelet Moments

The definition of B spline wavelets on a bounded interval and its construction, as well as its Mallat algorithm are shown in [16]. Based on these, new B spline interval wavelet moments descriptors are presented. Meanwhile the time complexity of the new descriptors is discussed.

3.1 B Spline Interval Wavelets and Its Filters

Definition 2 *Let* $\mathbf{t}_m^{(j)} := \{t_k^{(j)}\}_{k=-m+1}^{2^j+m-1}$, *with*

$$\begin{aligned} t_{-m+1}^{(j)} = t_{-m+2}^{(j)} = \cdots = t_0^{(j)} = 0,\\ t_k^{(j)} = k2^{-j}, \quad k = 1,\cdots,2^j-1,\\ t_{2^j}^{(j)} = t_{2^j+1}^{(j)} = \cdots = t_{2^j+m-1}^{(j)} = 1, \end{aligned}$$

be a knot sequence of mth order B splines on [0, 1] for any $j \in \mathbf{N}$.

For this knot sequence, B splines are defined as

$$B_{m,i}^j(x) := (t_{i+m}^{(j)} - t_i^{(j)})[t_i^{(j)}, t_{i+1}^{(j)}, \cdots, t_{i+m}^{(j)}]_t(t-x)_+^{m-1},$$

where $[\cdot,\cdots,\cdot]_t$ is mth divided difference of $(t-x)_+^{m-1}$ with respect to the variable t. We remark that

$$\text{supp}B_{m,i}^j = [t_i^{(j)}, t_{i+m}^{(j)}]$$

and

$$B_{m,i}^j(x) = N_m(2^j x - i), i = 0,\cdots,2^j - m,$$

where $N_m(x) := m[0,1,\cdots,m]_t(t-x)_+^{m-1}$ is the cardinal B spline of order m, while for $i = -m+1,\cdots,-1$, $B_{m,i}^j(x)$ contains a multiple knot at point 0 and for $i = 2^j - m + 1,\cdots,2^j - 1$ a multiple knot at point 1.

For the Chui-Wang B spline wavelets ψ_m, the following fact was established in [1]:

$$\begin{aligned}\psi_i^j(x) : &= \psi_m(2^j x - i)\\ &= \frac{1}{2^{2m-1}}\sum_{k=0}^{2m-2}(-1)^k N_{2m}(k+1)B_{2m,2i+k}^{j+1,(m)}(x),\end{aligned}$$

where $B_{2m,2i+k}^{j+1,(m)}(x)$ is the mth derivative function of $B_{2m,2i+k}^{j+1}(x)$. As

$$\text{supp}\psi_i^j = \left[\frac{2i}{2^{j+1}}, \frac{2i+4m-2}{2^{j+1}}\right],$$

we have

$$\text{supp}\psi_i^j \subseteq [0,1], \text{for } i = 0,\cdots,2^j - 2m + 1.$$

Hence on all levels j with $2^j \geq 2m-1$, at least one, now we called inner wavelet, exists whose support lies completely in [0, 1]. Let $j_0 \in \mathbf{N}$ be the smallest number which satisfies

$$2^{j_0} \geq 2m - 1.$$

Here we have $2m-2$ boundary wavelet, and for the reason of symmetry, 1 boundary wavelet can obtain from 0 boundary wavelet by an index transformation $i \to 2^{j_0} - 2m + 1 - i$. The 0 boundary wavelets are

$$\begin{aligned}\psi_i^{j_0}(x) : &= \frac{1}{2^{2m-1}}\Bigg[\sum_{k=-m+1}^{-1}\alpha_{i,k}B_{2m,k}^{j_0+1,(m)}(x)\\ &+ \sum_{k=0}^{2m-2+2i}(-1)^k N_{2m}(k+1-2i)B_{2m,k}^{j_0+1,(m)}(x)\Bigg], \quad i = -m+1,\cdots,-1,\end{aligned}$$

It can be shown [1] that the coefficients $\{\alpha_{i,k}\}_{k=-m+1}^{-1}$ are the solution of the $m-1$ linear systems of equations

$$\mathbf{B}\alpha_i = \mathbf{r}_i, \quad i = -m+1,\cdots,-1,$$

where $i, l = -m+1,\cdots,-1$,

$$\mathbf{B} := (b_{l,k})_{l,k=1}^{m-1}, \qquad b_{l,k} := B_{2m,-m+k}^{j_0+1}(t_l^{(j_0)}),$$

$$\mathbf{r}_i := (r_{i,-m+1},\cdots,r_{i,-1})^T,$$

$$r_{i,l} := -\sum_{k=0}^{2m-2+2i}(-1)^k N_{2m}(k+1-2i)N_{2m}(2m+2l-k),$$

$$\alpha_i := (\alpha_{i,-m+1}, \cdots, \alpha_{i,-1})^T.$$

Based on these, the scaling and wavelet functions are

$$\phi_k^j(x) = \begin{cases} B_{m,k}^{j_0}(2^{j-j_0}x), & k = -m+1, \cdots, -1, \\ B_{m,2^j-m-k}^{j_0}(1-2^{j-j_0}x), & k = 2^j-m+1, \cdots, 2^j-1, \\ N_m(2^j x - k), & k = 0, \cdots, 2^j - m. \end{cases}$$

$$\psi_k^j(x) = \begin{cases} \psi_k^{j_0}(2^{j-j_0}x), & k = -m+1, \cdots, -1, \\ \psi_{2^j-2m+1-k}^{j_0}(1-2^{j-j_0}x), & k = 2^j-2m+2, \cdots, 2^j-m, \\ \psi_m^{j_0}(2^j x - k), & k = 0, \cdots, 2^j - 2m + 1. \end{cases}$$

The dual scaling and wavelet functions are satisfied

$$< \tilde{\phi}_k^j, \phi_{k'}^j >= \int_0^1 \tilde{\phi}_k^j(x)\overline{\phi_{k'}^j(x)}dx = \delta_{kk'},$$

$$< \tilde{\psi}_k^j, \psi_{k'}^j >= \int_0^1 \tilde{\psi}_k^j(x)\overline{\psi_{k'}^j(x)}dx = \delta_{kk'}, \quad k, \quad k' = -m+1, \cdots, 2^j-1$$

Meanwhile

$$\tilde{\phi}_k^j(x) = \sum_{l=-m+1}^{2^j-1} g_{k,l}^j \phi_l^j(x), \quad k = -m+1, \cdots, 2^j-1$$

$$\tilde{\psi}_k^j(x) = \sum_{l=-m+1}^{2^j-m} h_{k,l}^j \phi_l^j(x), \quad k = -m+1, \cdots, 2^j-m$$

with $\mathbf{g_k^j} := (g_{k,-m+1}^j, g_{k,-m}^j, \cdots, g_{k,2^j-1}^j)^T, \mathbf{h_k^j} := (h_{k,-m+1}^j, h_{k,-m}^j, \cdots, h_{k,2^j-m}^j)^T$. That is

$$\mathbf{g}_k^j = (\mathbf{C}^j)^{-1}\mathbf{e}_k,$$

$$\mathbf{h}_k^j = (\mathbf{D}^j)^{-1}\mathbf{e}_k,$$

where

$$\mathbf{C}^j := (c_{k,l}^j)_{k,l=-m+1}^{2^j}, \quad c_{k,l}^j :=< \phi_k^j, \phi_l^j >,$$

$$\mathbf{D}^j := (d_{k,l}^j)_{k,l=-m+1}^{2^j-m}, \quad d_{k,l}^j :=< \psi_k^j, \psi_l^j >,$$

$\mathbf{e}_k$ is kth unit vector and

$c_{k,l}^j = 0$, if $|k-l| > m-1, d_{k,l}^j = 0$, if $|k-l| > 2m-2$.

Then the two-scale equations are

$$\phi_k^j(x) = \sum_{l=-m+1}^{2^{j+1}-1} p_{k,l}^j \phi_l^{j+1}(x), \quad k = -m+1, \cdots, 2^j-1,$$

$$\psi_k^j(x) = \sum_{l=-m+1}^{2^{j+1}-1} q_{k,l}^j \phi_l^{j+1}(x), \quad k = -m+1, \cdots, 2^j-m,$$

where $p_{k,l}^{j}$, $q_{k,l}^{j}$ are the low-pass and high-pass filters. Taking inner products with $\tilde{\phi}_{k}^{j+1}(x$

$$
\begin{aligned}
g1[0] &= \sum_{j=0}^{5} f[j] * q0[j];\\
g1[1] &= \sum_{j=0}^{7} f[j] * q1[j];\\
g1[i] &= \sum_{j=0}^{7} f[2i-2+j] * q[j], i = 2, 3, \cdots, 2^{N-1}-1;\\
g1[2^{N-1}] &= f[2^N] * q0[0] + f[2^N-1] * q0[1] + f[2^N-2] * q0[2];\\
g1[2^{N-1}+1] &= f[2^N+1] * q1[0] + f[2^N] * q1[1].
\end{aligned}
$$

3.2 B Spline Interval Wavelet Moments Descriptors for 3D Objects

In this way, by introducing B spline interval filters in 3D wavelet moments, we decompose the $S_{lm}(r)r^2$ in different level with the Mallat decomposition algorithm. Then combining the low-pass and high-pass signals, we get new descriptors for 3D object.

Definition 3 *For each object $f(r, \phi, \theta)$ expressed in polar coordinate and defined on field Ω, compute equation (3). Suppose the B spline interval wavelet degree is b, the sample number of one dimensional signal $S_{lm}(r)r^2$ is 2^N, and decompose the sampling signal with Mallat algorithm into M levels. Suppose $J = N - M$, they must satisfy $2^J \geq 2b - 1$. Put the decomposed signals together, we get*

$$C^{i,l}_{-J,k}, C^{l}_{-J,k}, D^{i,l}_{-j,k}, D^{l}_{-j,k}, i = 0, 1, J \leq j \leq N-1, l = 0, 1, 2, \cdots, L-1, k \in \mathbb{N},$$

where $C^{i,l}_{-J,k}$ is the L^2 norm of the vector $\mathbf{c}^{i,l}_{-J,k} = (c^{i,l,l}_{-J,k}, c^{i,l,l-1}_{-J,k}, \cdots, c^{i,l,-l}_{-J,k})^T$, and $\{C^{i,l,m}_{-J,k}\}_{k\in\mathbf{Z}}$ is the ith edge low-pass coefficients of signal $S_{lm}(r)r^2$ in level J. Like $C^{i,l}_{-J,k}$, the other three $C^{l}_{-J,k}, D^{i,l}_{-j,k}, D^{l}_{-j,k}$ are the interval (or edge) low pass (or high pass) coefficients. Then we call the vector

$$\{C^{i,l}_{-J,k}, C^{l}_{-J,k}, D^{i,l}_{-j,k}, D^{l}_{-j,k}\}_{i,j,l,k}$$

B spline interval wavelet moments descriptors.

Remark: The dimension of the descriptors is $2^N * L$.

3.3 Time Complexity

The time complexity of our new descriptors will be discussed by comparing with 3D wavelet moments descriptors. Because the real difference focuses on the radial integral, we only consider the time complexity of the one dimension signal $S_{lm}(r)r^2$. That is to compare them in a certain phase (l, m). Here $\psi(r)$ in 3D wavelet moments can be any wavelet function. In fact many different filters can be used to get the descriptors. While in 3D wavelet moments [3], the cubic B spline wavelet function is used, whose Gauss approximation form is

$$\psi(r) = \frac{4a^{d+1}}{\sqrt{2\pi(d+1)}} \cdot \sigma_\omega \cdot \cos(2\pi f_0(2r-1)) \cdot \exp\left(-\frac{(2r-1)^2}{2\sigma^2_\omega(d+1)}\right),$$

where $a = 0.697066$, $f_0 = 0.409177$, $\sigma_\omega^2 = 0.561145$, $d = 3$, $p = 0, 1, 2, 3 \cdots$, $q = 0, 1, 2, \cdots, 2^{m+1}$.

According to this background, we discuss the time complexity of 3D wavelet moments with cubic B spline wavelets and the interval wavelet moments with B spline wavelets. Suppose the sampling number is 2^N, M is the maximum number of q in wavelet moments, and that of the decomposition level number of B spline interval wavelet moments. The maximum length of interval B spline low-pass and high-pass filers is n.

1. The computation of the 3D wavelet moments descriptors (wavelet function is cubic B-spine) is about $(2^{M+2} + M - 1)2^N \cos(\cdot) \exp(\cdot)$, where we must compute two complex functions. The dimension of the descriptors is $2^{M+2} + M - 1$.

2. The computation of all wavelet coefficients of M level in the interval B spline wavelet moments is about $(2^{N+1} - 2^{N-M+1}) * n$. The dimension of the descriptors is 2^N.

The computation complexity of the B spline interval wavelet moments descriptor is faster than the wavelet moments when the decomposition level M is larger.

4 Experiments

In the experiments, we use the 3D model database from the Princeton Shape Benchmark [17]. We use a database including 149 models (69 chairs and 80 planes), shown in Fig. 1. By precision-recall curve, we compare different descriptors with different measure, see Figs. 2–4.

Wavelet moments descriptors with cubic B spline wavelets (Wav), Wavelet moments descriptors with Db3 wavelet (Db), interval wavelet moments descriptors corresponding to Db3 (InterWav), interval wavelet with B spline wavelets (m=3) (BInterWav) and these four methods with Pearson distance (pWav, pDb, pInterWav, pBInterWav) are our main methods to simulate the 3D model retrieval system. Given a test model in the database, we sort others by the similarity to the model. All 3D objects in our database are normalized to be 1 m^3. The filters are listed in Table 1.

Moreover other parameters are the sampling number $N = 6$, harmonic function parameter $L = 8$ and decomposition level $M = 4$. The dimension of the wavelet moments with cubic B spline wavelets descriptors is 538. The dimension of the other methods are the same 512.

In our experiment, we use the Euclidean distance and our Pearson distance to measure the similarity of two descriptors for two objects. Our Pearson distance is put forward by weighted Pearson correlation coefficient together with their energy in every level.

The definition of Pearson correlation coefficient of vectors x and y is

$$r = \frac{\sum(x - \bar{x})(y - \bar{y})}{\sqrt{\sum(x - \bar{x})^2}\sqrt{\sum(y - \bar{y})^2}}$$

where $\bar{x}$ and $\bar{y}$ are the average of n-dimension vector x and y [8].

The correlation coefficient is a number between -1 and $+1$ that measures the degree of association between two variables x and y. A positive value for the correlation implies a positive association (large values of x tend to be associated with large values of y and small values of x tend to be associated with small values of y). A negative value for the correlation implies a

negative or inverse association (large values of x tend to be associated with small values of y and vice versa). It characterize not their absolutely size but their change direction. It is useful to

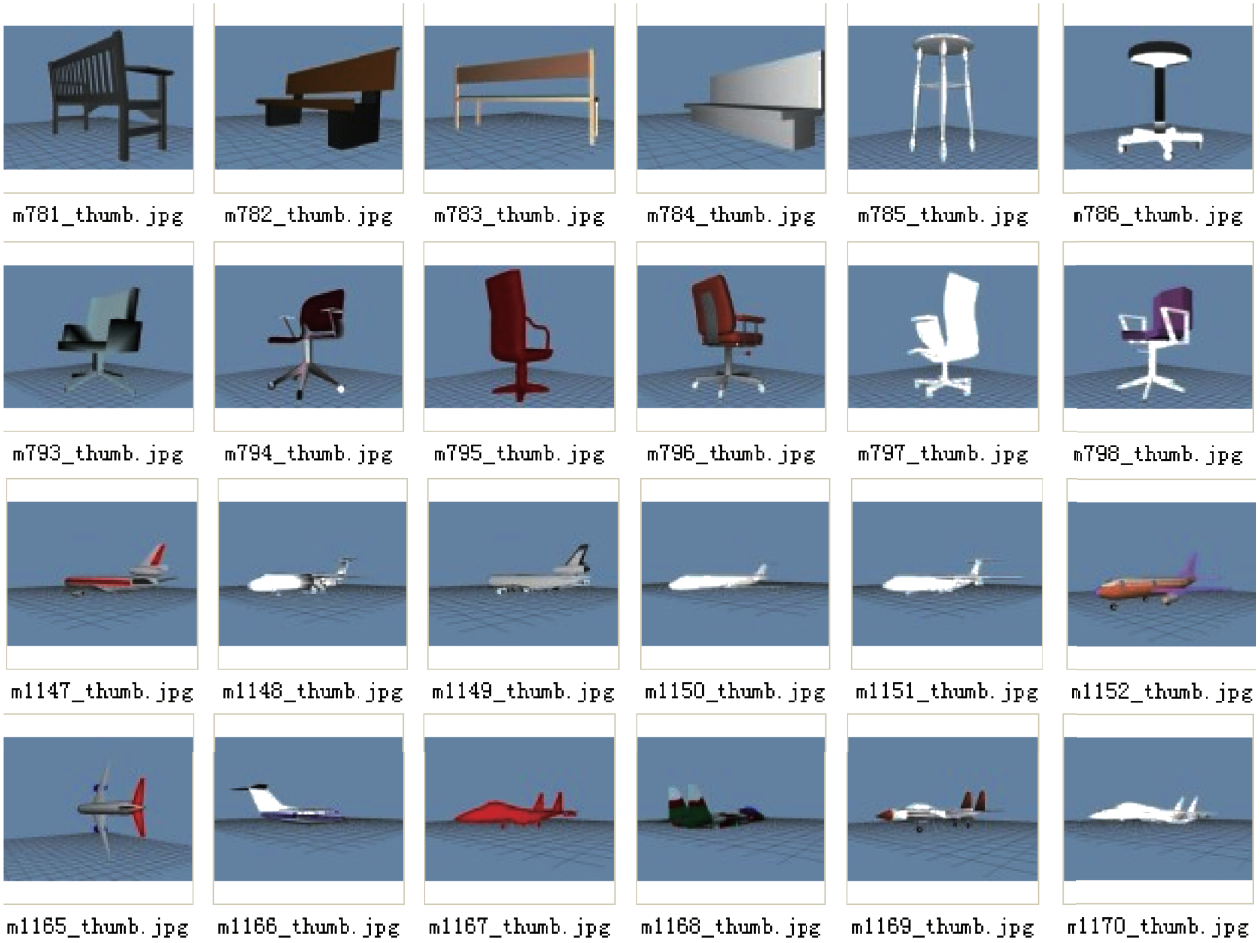

Fig. 1: Several 3D models in our database

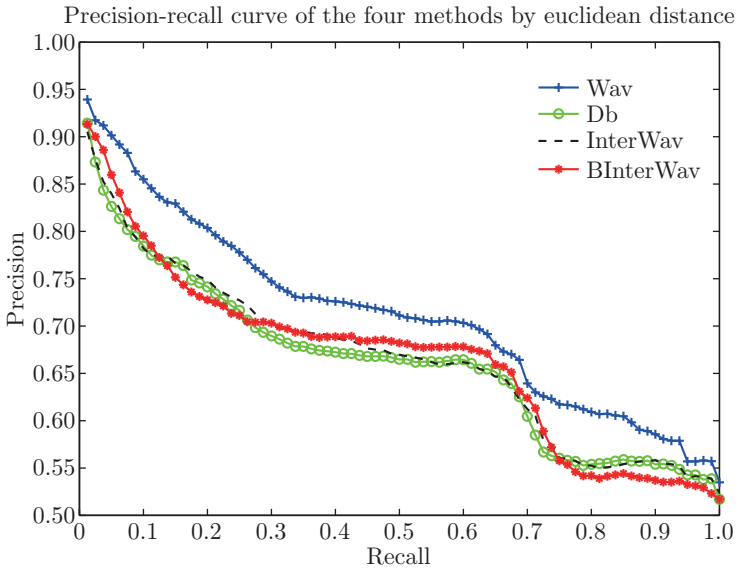

Fig. 2: Precision-Recall curve of the four retrieval methods by Euclid distance

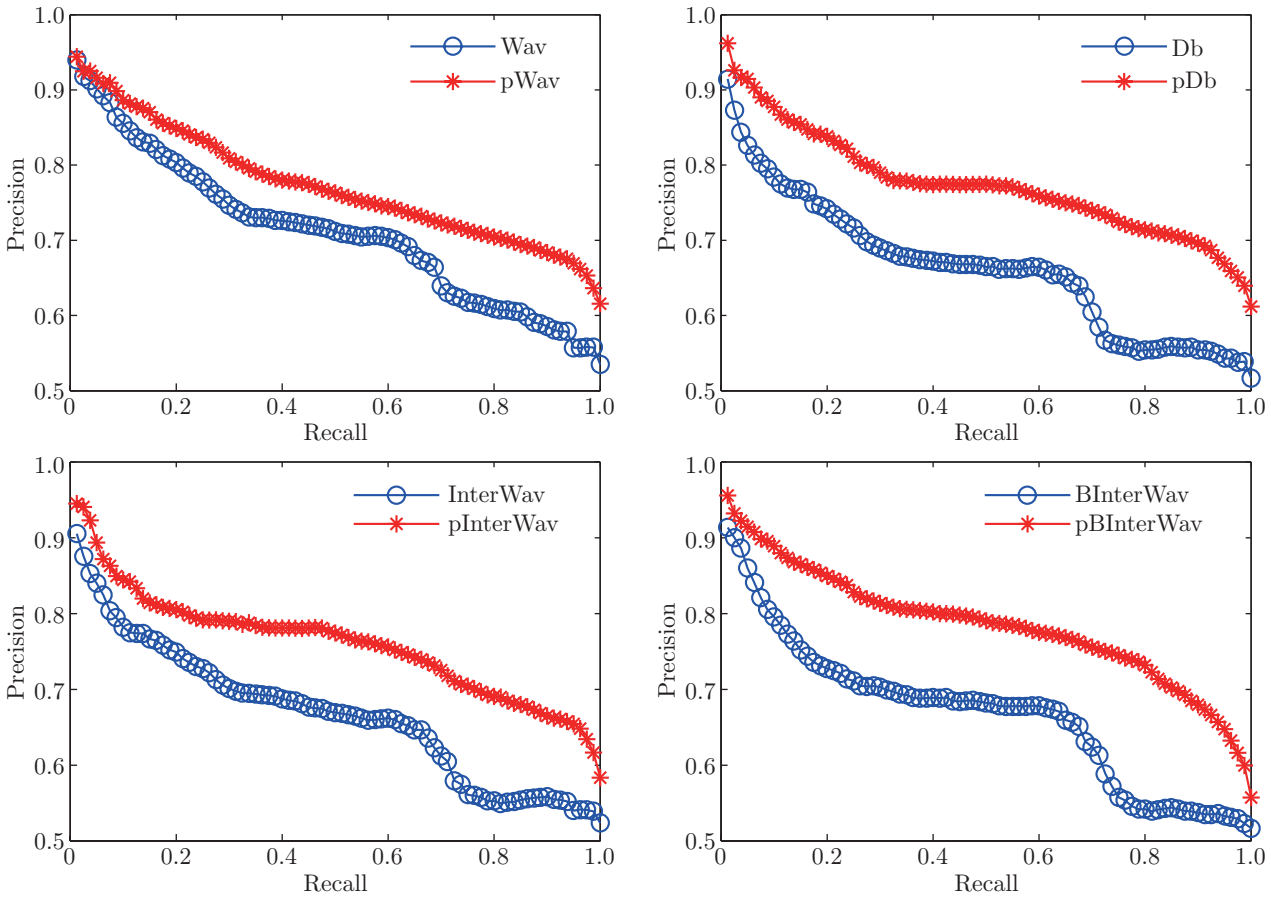

Fig. 3: Precision-Recall curves of the four retrieval methods by Euclidean distance and Pearson distance respectively

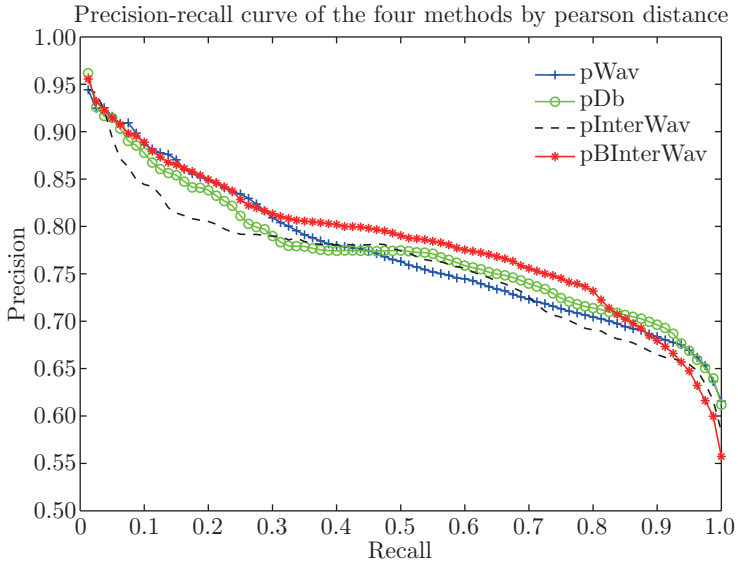

Fig. 4: Precision-Recall curve of the four retrieval methods by Pearson distance

measure the similarity of two level descriptors.

Furthermore the energy of two descriptors is also important to character the objects. So we

use Er to measure the energy similarity, which is defined by

$$Er = 1 - \frac{|\|x\| - \|y\||}{max(\|x\|, \|y\|)}$$

where $max(\|x\|, \|y\|)$ means the maximum of the norms of x and y. Er is a number between 0 and 1. Large value of Er means the two objects more similar in energy.

$c_r^{j,l}$ and $d_r^{j,l}$ respectively denote the Pearson correlation coefficient of the low-pass part and high-pass part of two objects in (j,l)th level, where $N - M \leq j \leq N - 1, l = 0, \cdots, L$. R_l is the whole Pearson correlation coefficient of two descriptors in lth level, where $l = 0, \cdots, L$. Then the similarity of two objects is defined by

$$Q = \frac{\sum_{l=0}^{L} Er_l * \left(\frac{2^M * c_r^{N-M,l} + 2^M * d_r^{N-M,l} + 2^{M-1} * d_r^{N-M+1,l} + \cdots + 2 * d_r^{N-1,l}}{2^M + 2^M + 2^{M-1} + \cdots + 2} + 2 * R_l \right)}{3 * (L+1)}$$

We call it Pearson distance of two object. The larger value of Q means more similarity of two objects.

In Euclidean distance, the wavelet moments is better than the other three methods in Fig. 2. However in Fig. 3, the Pearson distance is more suitable to character the similarity of this kind of level descriptors. It gets higher precision and recall curve of every descriptor method. At last, from the results in Fig. 4, we can see the interval B spline wavelet moments descriptor with Pearson distance is better than the other methods in high precision rate. It is true because the interval wavelet emphasize the edge of objects. Furthermore the average times of the two methods are shown in Table 2 (CPU 2.50 GHz, 1 G memory). Compared with the original wavelet moments descriptors, the interval B spline wavelet moments descriptors have some advantage in time complexity.

Table 2: Time cost of the Wav and BInterWav descriptors

Time	Wav	BInterWav
Second	34.626	26.384

5 Conclusion and Future Work

In this paper, we propose interval B spline wavelet moments descriptors of 3D objects. We evaluate it in a middle database and test the effect of the new method. From the experiments, by introducing the interval B spline wavelets and Pearson correlation coefficient, we improve the wavelet moments method in 3D retrieval system. Compared with wavelet moments, interval B spline wavelet moments descriptors has simple computation, which is very favorable for large 3D system database recognition. Furthermore, when we extract multi-level fractal features from coarsely to finely, the performance may be improved to some extent.

In the future experiment on a bigger database and more changes will be done to test our method. Furthermore we can try to use different clustering methods to classify 3D objects by our descriptors.

Acknowledgement

The authors would sincerely thank Professor Hua Li and Doctor Dong Xu, who give some meaningful advices.

References

[1] C. K. Chui, E. Quak, Wavelets on a bounded interval, in Numerical Methods of Approximation Theory, Vol. 9 (D. Brass and L. L. Schumaker, Eds.), 1992, 53-75

[2] A. Cohen, I. Daubechies, Wavelets on the interval and fast wavelet transforms, Applied and Computational Harmonics Analysis, 1 (1993), 54-81

[3] L. Cui, H. Li, Z. Li, Y. Wang, Y. Liu, 3-D discriminative wavelet moment descriptors for 3-D objects, in: Proc. Wavelet Analysis and Its Applications, 2004, 70-75

[4] L. Cui, H. Li, A new combined fractal scale descriptor for gait sequence, in: Proc. Machine Learning and Data Mining, 2007, 616-627

[5] L. Cui, Y. Li, D. Xu, H. Li, Fractal scale descriptors based on 3D wavelet moments for 3D objects, in: Proc. Wavelet Analysis and Pattern Recognition, 2007, 1127-1133

[6] L. Cui, Y. Li, H. Li, 3D interval wavelet moments for 3D objects, Jounal of Information and Computational Science, 6(4), 2009, 1799-1810

[7] M. K. Hu, Visual pattern recognition by moment invariants, IRE Trans. Inform. Theory, 8 (1962), 179-187

[8] L. Jan, Introduction and Univariate Descriptive Statistics, http://www.stat.tamu.edu/stat30x/notes/node4.html, 1996

[9] M. Kazhdan, B. Chazelle, D. Dobkin, T. Funkhouser, S. Rusinkiewicz, A reflective symmetry descriptor for 3D models, in: Proc. European Conference on Computer Vision, 2002, 642-656

[10] D. V. Vranid, D. Saupe, 3D shape descriptor based on 3D fourier transform, in Proc. Multimedia Communications and Services of IEEE EURASIP Conference on Digital Signal Processing, 2001, 271-274

[11] M. Kazhdan, T. Funkhouser, S. Rusinkiewicz, Rotation invariant spherical harmonic representation of 3D shape descriptors, in: Proc. Symposium on Geometry Processing, 2003, 156-164

[12] M. J. Mohlenkamp, A User's Guide to Spherical Harmonics, http://www.math.ohiou.edu/mjm/research/uguide.pdf, 2007

[13] M. Novotni, R. Klein, 3D Zernike descriptors for content based shape retrieval, in: Proc. ACM Symposium on Solid Modeling and Applications, 2003, 216-225

[14] G. Zhao, L. Cui, H. Li, Gait recognition using fractal scale, Pattern Analysis & Applications, 10(3), 2007, 235-246

[15] R. Osada, T. Funkhouser, B. Chazelle, D. Dobkin, Matching 3D models with shape distributions, in: Proc. Shape Modeling and Applications, 2001, 154-167

[16] E. Quak, N. Weyrich, Decomposition and reconstruction algorithms for spline wavelets on a bounded interval, Applied and Computational Harmonics Analysis, 1 (1994), 217-231

[17] P. Shilane, P. Min, M. Kazhdan et al., The princeton shape benchmark, in: Proc. Shape Modeling International, 2004, 167-178